

On the uncertainty estimates of the σ -pole determination by Padé approximants

Irinel Caprini,¹ Pere Masjuan,² Jacobo Ruiz de Elvira,³ and Juan José Sanz-Cillero⁴

¹*Horia Hulubei National Institute for Physics and Nuclear Engineering,
P.O.B. MG-6, 077125 Bucharest-Magurele, Romania*

²*PRISMA Cluster of Excellence, Institut für Kernphysik,
Johannes Gutenberg-Universität, D-55099 Mainz, Germany*

³*Helmholtz-Institut für Strahlen- und Kernphysik, Universität Bonn, D-53115 Bonn, Germany*

⁴*Departamento de Física Teórica and Instituto de Física Teórica,
IFT-UAM/CSIC Universidad Autónoma de Madrid, Cantoblanco, Madrid, Spain*

We discuss the determination of the $f_0(500)$ (or σ) resonance by analytic continuation through Padé approximants of the $\pi\pi$ -scattering amplitude from the physical region to the pole in the complex energy plane. The aim is to analyze the uncertainties of the method, having in view the fact that analytic continuation is an ill-posed problem in the sense of Hadamard. Using as input a class of admissible parameterizations of the scalar-isoscalar $\pi\pi$ partial wave, which satisfy with great accuracy the same set of dispersive constraints, we find that the Roy-type integral representations lead to almost identical pole positions for all of them, while the predictions of the Padé approximants have a larger spread, being sensitive to features of the input parameterization that are not controlled by the dispersive constraints. Our conservative conclusion is that the σ -pole determination by Padé approximants is consistent with the prediction of Roy-type equations, but has an uncertainty almost a factor two larger.

PACS numbers: 11.55.Bq, 11.55.Fv, 14.40.Be

I. INTRODUCTION

The determination of a broad resonance like the $I = J = 0$ lowest state $f_0(500)$ (known also as σ) is a notoriously difficult problem. The associated S -matrix pole is situated deep in the complex energy plane and, until recent years, the knowledge of $\pi\pi$ scattering at low energies was poor. Therefore, the extraction of the σ -resonance parameters was affected by large errors. For some time, the very existence of this resonance was doubted. The predictions quoted in the current version of PDG [1] still cover a large range, although reduced compared to the previous editions. A thorough review of the history of the $f_0(500)$ resonance can be found in the recent paper [2].

The lack of precision in the early determinations of the σ resonance can be related to a great extent to the fact that analytic continuation is an ill-posed or unstable problem in the Hadamard sense [3], *i.e.* arbitrarily small changes in the input data may lead to indefinitely large variations in the solution. Therefore, analytic functions which are very close along a finite range in the complex plane may differ arbitrarily much outside it¹. In the case of the σ resonance, the phenomenon is manifest in a dra-

matic way because the pole is located far from the physical region and until recent years no accurate data on $\pi\pi$ scattering at low energies were available.

A major progress was achieved by the use of Chiral Perturbation Theory and dispersion theory, which led to a precise theoretical description of $\pi\pi$ scattering at low energies [5, 6]. In particular, Roy equations [7], which fully exploit analyticity, unitarity and crossing symmetry of the $\pi\pi$ scattering amplitude, are a set of coupled integral equations, whose solutions yield precise values of the partial waves at low energies. At the same time, Roy equations provide integral representations which allow the calculation of the partial waves at complex points in a certain domain of the first Riemann sheet. The input available along both the right and left cuts by crossing symmetry ensures the stability of the extrapolation to points inside the holomorphy domain. This allowed a first precise determination of the mass and width of σ resonance, reported in [8]:

$$m_\sigma = 441_{-8}^{+16} \text{ MeV}, \quad \Gamma_\sigma/2 = 272_{-12.5}^{+9} \text{ MeV}. \quad (1)$$

A similar calculation performed in [9] confirmed this result, with a somewhat smaller error due to a less conservative estimate of the uncertainties of the input phase-shifts near 800 MeV.

Further studies of Roy equations and of their once-subtracted version, known as GKPY equations, were performed in [10], including also recent data at low energies from the NA48 experiment [11]. The σ -pole parameters

¹ Examples of instability of analytic continuation and its pitfalls in particle physics have been discussed for the first time in [4].

based on GKPY equations read [12]:

$$m_\sigma = 457_{-13}^{+14} \text{ MeV}, \quad \Gamma_\sigma/2 = 279_{-7}^{+11} \text{ MeV}. \quad (2)$$

Recently, a result with a comparable precision was reported in [13]:

$$m_\sigma = 453 \pm 15 \text{ MeV}, \quad \Gamma_\sigma/2 = 297 \pm 15 \text{ MeV}. \quad (3)$$

This result was obtained using a method based on Padé approximants (PA) for performing the analytic continuation from the physical region to the pole on the second Riemann sheet [14]. As starting point for constructing the Padé approximants, a specific parameterization of the scalar isoscalar $\pi\pi$ partial wave at low energies, given in [10], was used. The parameterization satisfies with great accuracy Roy and GKPY equations, being therefore a suitable input. However, it might be possible to find different parameterizations which satisfy to the same extent the analyticity constraints as the one adopted in [13] and may lead to different σ -pole parameters. Choosing only one parameterization might lead to an underestimate of the true uncertainty of the method.

In the present paper we investigate the uncertainty of the σ -pole determination by considering a larger class of functions used as starting point in the construction of the Padé approximants. Our approach is similar to the analysis performed in [15], where it was shown that the direct analytic continuation of specific parameterizations cannot compete with Chiral Perturbation Theory and Roy equations in the precise determination of the pole associated to the σ resonance. However, while in [15] the free parameters were fixed by fitting the experimental data on the $\pi\pi$ phase shifts available at low energies, in the present paper we require that the parameterizations satisfy to a great accuracy a set of dispersive constraints. By extrapolating the Padé approximants of these amplitudes to the σ pole, as in Ref. [13], we assess in a more realistic way the uncertainty of the pole prediction by this method. The reliable estimate of the error of the Padé method will be useful in situations where the determination of resonance poles is not accessible with Roy or GKPY equations, like in $\pi\pi$ scattering.

The plan of the paper is as follows: in the next section we describe the class of admissible amplitudes used in our study. In Sec. III we determine the free parameters of the input parameterizations and their statistical uncertainties by imposing the set of dispersive constraints considered in [10]. In Secs. IV and V we calculate the pole parameters of the σ resonance for the class of admissible functions, using their contribution to the integral dispersive representations and their Padé approximants, respectively, and discuss also the statistical and systematic errors of the predictions. The last section contains a summary and our conclusions.

II. CLASS OF ADMISSIBLE AMPLITUDES

We consider the $I = J = 0$ $\pi\pi$ partial wave $t_0^0(s)$, which is known to be a real-analytic function in the s -complex plane cut for $s \leq 0$ and $s \geq 4m_\pi^2$ and has a so-called Adler zero at $s \approx m_\pi^2/2$. On the elastic region of the right cut, which extends to a good approximation up to the $K\bar{K}$ -production threshold, the function $t_0^0(s)$ is expressed as

$$t_0^0(s) = \frac{e^{2i\delta_0^0(s)} - 1}{2i\rho(s)}, \quad (4)$$

where $\rho(s) = \sqrt{1 - 4m_\pi^2/s}$ and $\delta_0^0(s)$ is the phase shift. This relation implies the elastic unitarity relation

$$\text{Im} \left[\frac{1}{t_0^0(s + i\epsilon)} \right] = -\rho(s), \quad (5)$$

which is valid for $4m_\pi^2 \leq s < 4m_K^2$. Therefore, if $t_0^0(s)$ is expressed in general as

$$t_0^0(s) = \frac{1}{\psi(s) - i\rho(s)}, \quad (6)$$

from (5) it follows that the function $\psi(s)$ is real on the elastic region, where it has the expression

$$\psi(s) = \rho(s) \cot \delta_0^0(s), \quad 4m_\pi^2 \leq s < 4m_K^2. \quad (7)$$

The reality property implies also that $\psi(s)$ is analytic in the s -plane cut for $s \leq 0$ and $s \geq 4m_K^2$, except for the Adler pole at $s = z_0^2/2$, $z_0 \approx m_\pi$. The parameterization of the partial wave adopted in [10] improves the so-called ‘‘effective-range approximation’’, which amounts to expanding $\psi(s)$ in powers of k^2 , where $k = 1/2\sqrt{s - 4m_\pi^2}$ is the c.m. momentum. It uses the conformal mapping

$$w(s) = \frac{\sqrt{s} - \sqrt{4m_K^2 - s}}{\sqrt{s} + \sqrt{4m_K^2 - s}}, \quad (8)$$

which maps the s plane cut for $s \leq 0$ and $s \geq 4m_K^2$ onto the unit disc $|w| < 1$ in the plane $w \equiv w(s)$. Then the expansion in powers of $w(s)$ of the form

$$\psi(s) = \frac{m_\pi^2}{s - \frac{1}{2}z_0^2} \times \left\{ \frac{z_0^2}{m_\pi\sqrt{s}} + B_0 + B_1w(s) + B_2w(s)^2 + B_3w(s)^3 \right\}, \quad (9)$$

defined as in Eqs. (A1)-(A2) of [10], converges in a larger domain and has a better convergence than the simple expansion in powers of k^2 . We note that the first term in the second line of (9) removes the singularity of $\rho(s)$ at $s = 0$ in the denominator of (6). The parameters B_n of the expansion (9) were taken from the so-called ‘‘CFD parameterization’’ of the $\pi\pi$ partial waves, given in Table V of [10], which we will describe in detail in Sec. III. In Refs. [10, 13], the parameterization (9) was adopted in

the range $4m_\pi^2 \leq s \leq s_M$, with $\sqrt{s_M} = 0.85$ GeV. In this paper we shall denote this parameterization of the S_0 partial wave as v_1 .

We can construct other parameterizations by using in the expansion (9), instead of the conformal mapping (8), a more general mapping $w(s, \alpha)$, defined as:

$$w(s, \alpha) = \frac{\sqrt{s} - \alpha\sqrt{4m_K^2 - s}}{\sqrt{s} + \alpha\sqrt{4m_K^2 - s}}. \quad (10)$$

Then we write $\psi(s)$ as:

$$\psi(s) = \frac{m_\pi^2}{s - \frac{1}{2}z_0^2} \times \left\{ \frac{z_0^2}{m_\pi\sqrt{s}} + B_0 + B_1w(s, \alpha) + B_2w(s, \alpha)^2 + B_3w(s, \alpha)^3 \right\}. \quad (11)$$

As discussed in Ref. [15], with a proper choice of α the region $(4m_\pi^2, s_M)$ is mapped onto an almost symmetrical range around the origin in the w plane, which ensures a better convergence of the expansion (11) compared to (9). For numerical purposes we will take $\alpha = 0.7$. The parameterization defined in this way is denoted as v_2 .

A somewhat different choice is the so-called Schenk parameterization [16], adopted in solving Roy equations in [5, 6, 8, 9, 17]. In our notations it corresponds to writing the function $\psi(s)$ entering (6) as

$$\psi(s) = \frac{1}{B_0 + B_1k^2 + B_2k^4 + B_3k^6} \frac{s - z_0^2}{4m_\pi^2 - z_0^2}, \quad (12)$$

where k is the c.m. momentum defined above. The free parameters are the coefficients B_n and z_0 . We denote this alternative parameterization as v_3 .

Other parameterizations are obtained using the Chew-Mandelstam procedure [18] of implementing the unitarity relation (5), based on a function which is analytic in the plane cut for $s \geq 4m_\pi^2$ and has the imaginary part on the cut equal to the factor $\rho(s)$. For convenience, we consider the loop function $\bar{J}(s)$, written as

$$\bar{J}(s) = \frac{2}{\pi} + \frac{\rho(s)}{\pi} \ln \left[\frac{\rho(s) - 1}{\rho(s) + 1} \right]. \quad (13)$$

It can be checked that this function vanishes at the origin, $\bar{J}(0) = 0$, and

$$\text{Im} \bar{J}(s + i\epsilon) = \rho(s), \quad s \geq 4m_\pi^2. \quad (14)$$

If one defines the function $\tilde{\psi}(s)$ by writing:

$$t_0^0(s) = \frac{1}{\tilde{\psi}(s) - \bar{J}(s)}, \quad (15)$$

the unitarity relation (5) and the equality (14) show that $\tilde{\psi}(s)$ is real for $4m_\pi^2 \leq s < 4m_K^2$, where it is related to the phase shift $\delta_0^0(s)$ by

$$\tilde{\psi}(s) = \rho(s) \cot \delta_0^0(s) + \text{Re} \bar{J}(s). \quad (16)$$

$t_0^0(s)$	Equations
v_1	(6), (9)
v_2	(6), (11)
v_3	(6), (12)
v_4	(15), (17)
v_5	(15), (18)

TABLE I: Summary of the equations used for the definition of the five parameterizations v_i adopted in the present work. The version v_1 is denoted as CFD in [10].

The reality property implies also that $\tilde{\psi}(s)$ is analytic in the s -plane cut for $s \leq 0$ and $s \geq 4m_K^2$, except for the Adler pole at $s = z_0^2/2$, and can be expanded as

$$\tilde{\psi}(s) = \frac{m_\pi^2}{s - \frac{z_0^2}{2}} [B_0 + B_1w(s) + B_2w(s)^2 + B_3w(s)^3], \quad (17)$$

in powers of the variable (8). We remark that the compensating term $\frac{z_0^2}{m_\pi\sqrt{s}}$ appearing in (9) is no longer necessary in (17), since the function $\bar{J}(s)$ is by definition regular at $s = 0$. This parameterization is labeled as v_4 .

In a similar way, we can expand the function $\tilde{\psi}(s)$ in powers of the more general conformal mapping $w(s, \alpha)$ defined in (10):

$$\tilde{\psi}(s) = \frac{m_\pi^2}{s - \frac{1}{2}z_0^2} \times [B_0 + B_1w(s, \alpha) + B_2w(s, \alpha)^2 + B_3w(s, \alpha)^3]. \quad (18)$$

For numerical purposes we will take $\alpha = 0.5$. The corresponding parameterization is denoted as v_5 .

We summarize in Table I the relations used for the definition of the five parameterizations considered in our analysis. As in [13], we have assumed that these expressions are valid on the real axis in the range $4m_\pi^2 \leq s \leq s_M$, with $\sqrt{s_M} = 0.85$ GeV. The free parameters were determined by requiring that the amplitude $t_0^0(s)$ satisfies with great precision the dispersive constraints on the $\pi\pi$ amplitude. This analysis is presented in the next section.

III. DISPERSIVE CONSTRAINTS ON THE ADMISSIBLE PARAMETERIZATIONS

During the last years, dispersion relations have proved to be a successful tool for describing with high precision different low-energy hadronic processes (for some examples see [5, 6, 8, 10, 19, 20]). Based on general principles such as Lorentz invariance, causality, unitarity and crossing symmetry, they allow for a rigorous formalism, which expresses a scattering amplitude at any energy point as a Cauchy integral over the whole energy range. The dispersive representations can provide information on the amplitude even at energies where data are poor, in unphysical regions or in the complex plane. Furthermore,

the formalism is model independent, in the sense that the details of the parameterizations used to describe the experimental data become irrelevant once they are used as input in the dispersive integrals.

For $\pi\pi$ scattering crossing symmetry implies further relations between the left- and right-hand cuts and makes this process specially suited to be analyzed using dispersive techniques. The comprehensive analysis performed in [10] was based on suitable $\pi\pi$ partial-wave parameterizations obtained from fits to experimental data, but constrained also to satisfy dispersion relations. In particular Forward Dispersion Relations (FDR), once and twice-subtracted Roy equations and two sum rules were imposed as further constraints to the experimental data fits. For completeness, we will summarize next the main characteristics of these dispersion relations.

FDR are fixed- t dispersion relations calculated at the forward or $t = 0$ direction [10]. They are written in a basis of $s \leftrightarrow t$ symmetric or antisymmetric amplitudes describing the processes $\pi^0\pi^0 \rightarrow \pi^0\pi^0$, $\pi^0\pi^+ \rightarrow \pi^0\pi^+$ and the amplitude corresponding to the process with isospin one in the t -channel. Standard Roy equations (RE) [7] are obtained from the partial wave projection of a twice-subtracted fixed- t dispersion relation, where the t -dependent subtraction terms are determined by $s \leftrightarrow t$ crossing symmetry. This leads to a coupled system of partial-wave dispersion relations (PWDRs), where the scattering lengths are the only free parameters that appear in the subtraction terms. Once subtracted Roy or GKPY equations were derived first in [10] and, compared to RE, proved to have a slower increase of the uncertainty as the energy grows, making them very well suited for constraining the $\pi\pi$ amplitude in the $f_0(500)$ region. Finally, two sum rules evaluated at threshold were used to constrain the t -dependent high-energy Regge behavior in terms of low-energy P - and D -wave parameters. The first one was constructed in the Pomeron channel whereas the second was defined for the ρ Reggeon exchange.

The determination of the $\pi\pi$ partial waves in [10] can be summarized as follow: first a set of simple expressions for each partial wave amplitude are considered to fit separately the available experimental data sets [11, 21, 22]. Each data set is checked against FDR and other two dispersive sum rules [10]. This leads to an Unconstrained Fit to Data (UFD), where only those experimental data sets compatible within uncertainties with dispersion relations are taken into account. A recent statistical analysis [23] has shown that this selection of the experimental data for the UFD violates only slightly the normality requirements of the residual distributions, which could be fulfilled with tiny modifications of the data selection, leading to almost identical results.

Finally, the parameterizations are used as a starting point for a Constrained Fit to Data (CFD), in which RE and GKPY, as well as FDR, are imposed as additional constraints. As a result, one obtains a set of consistent parameterizations which, describing the experimental data, also satisfy the dispersive constraints based on

analyticity, crossing symmetry and unitarity, and hence are much more precise and reliable.

The determination of the σ pole reported in [13] used the CFD parameterization of the $S0$ partial wave as input for the analytic extrapolation in the complex plane using Padé approximants. As discussed above, in order to determine the uncertainty of the method in a more exhaustive way, we will use now for the $S0$ -wave at low energies the whole class of parameterizations described in Sec. II.

The easiest way to ensure that the new parameterizations still satisfy the dispersive constraints imposed to the CFD is to determine their free parameters by minimizing the difference between the new $S0$ -wave curves and the CFD one at low energies. In addition, the errors of the parameters are fixed so that they reproduce the CFD $S0$ -wave error bands. The curves obtained in this way are shown in Fig. 1, whereas the final parameter values and errors are collected in Table II.

In order to check whether the new parameterizations are consistent or not with the dispersion relations, we use the method applied in [10]. We assume that each of the dispersion relations described above, namely the three FDR, Roy and GKPY equations and the two sum rules, denoted generically as a , is well satisfied at a point s_n , if the difference between its left-hand side and right-hand side (Δ_a) is smaller than its uncertainty ($\delta\Delta_a$), which is computed using a Monte Carlo sampling of all the parametrization parameters within 6 standard deviations. Thus, if the average discrepancy for a total number of points N verifies

$$\bar{d}_a^2 \equiv \frac{1}{N} \sum_n \left(\frac{\Delta_a(s_n)}{\delta\Delta_a(s_n)} \right)^2 \leq 1, \quad (19)$$

we consider that the dispersion relation a is well satisfied within uncertainties. Following the same convention considered in [10], the values of $s_n^{1/2}$ are taken at intervals of 25 MeV between threshold and the maximum energy point defined in [10] (1420 MeV for the FDR and 1115 MeV for GKPY equations). The \bar{d}_a^2 values obtained for each dispersion relation and parameterization are collected in Table III, and prove that all parameterizations satisfy the dispersion relations equally well. Hence, they are perfectly admissible as input for the Padé approximants in order to extract the $f_0(500)$ -pole parameters.

IV. POLE DETERMINATION FROM GKPY EQUATIONS

The equations denoted as GKPY in [10] are a coupled system of partial-wave dispersion relations in which the unphysical left-hand cut is rewritten as a series of integrals over the right-hand cut, thus expressing the partial waves at any point in the complex plane as integrals along the physical region involving only observable quantities.

	v_1	v_2	v_3	v_4	v_5
B_0	7.1 ± 0.2	10.7 ± 0.5	0.22 ± 0.01	0.36 ± 0.02	14.9 ± 0.5
B_1	-25.4 ± 0.5	-15.3 ± 0.3	$(13.9 \pm 0.3) \text{ GeV}^{-2}$	-59.0 ± 0.7	-22.2 ± 0.9
B_2	-33.2 ± 1.2	-22.5 ± 0.8	$-47.6 \pm 1.7 \text{ GeV}^{-4}$	-50.0 ± 1.2	-44.9 ± 1.6
B_3	-26.2 ± 2.3	-34.0 ± 2.9	$(-29.2 \pm 2.5) \text{ GeV}^{-6}$	1.04 ± 0.01	-44.0 ± 3.8
z_0	m_π	m_π	0.83 GeV	m_π	m_π

TABLE II: Values of the parameters of the different S_0 -wave expressions described in Sec. II. The choice v_1 coincides with the so-called ‘‘CFD’’ solution defined in [10].

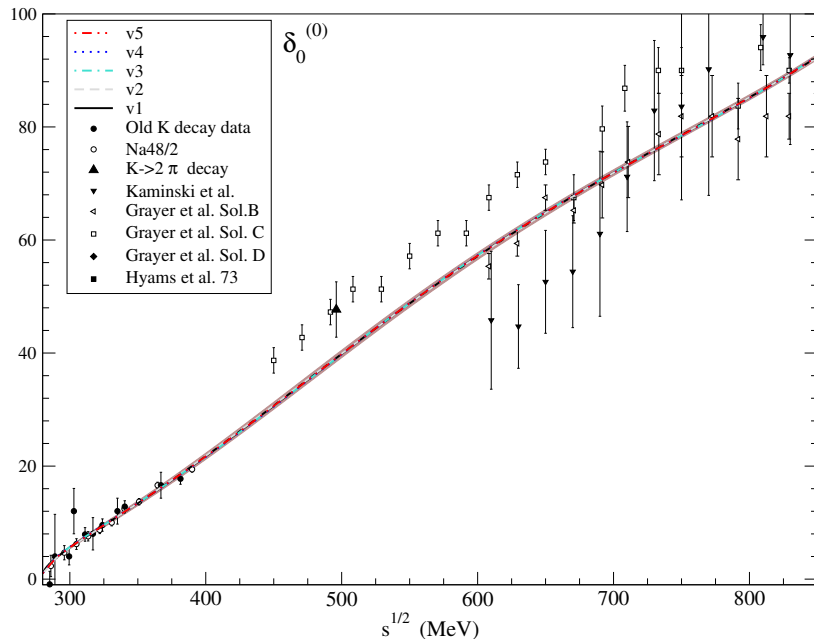


FIG. 1: $\pi\pi$ S_0 -wave phase shift for each of the parameterizations discussed in Sec. II in the region between the $\pi\pi$ threshold and $\sqrt{s_M} = 0.85 \text{ GeV}$. The dark band covers the uncertainties of the v_1 (CFD) parameterization. The experimental data points [21, 22] correspond to those discussed in detail in [10].

The general form of these equations is

$$t_J^I(s) = k_J^I + \frac{1}{\pi} \int_{4m_{\pi^2}}^{\infty} ds' \sum_{I'=0}^2 \sum_{J'=0}^{\infty} K_{JJ'}^{II'}(s, s') \text{Im} t_{J'}^{I'}(s'), \quad (20)$$

where the subtraction terms k_J^I are just linear combinations of the isoscalar and isotensor scattering lengths a_0^I , and the kernels $K_{JJ'}^{II'}$ are composed of a singular Cauchy kernel and a regular remaining piece.

In contrast to the standard Roy equations [7], GKPY equations are constructed from a once-subtracted fixed- t dispersion relation, leading to the GKPY constant subtraction terms in (20). This produces a smooth error increase at higher energies, which makes them more suited for the study of the $f_0(500)$ energy region.

An extremely important feature of (20) is that the

Cauchy integrals only require as input the value of the partial waves on the boundary. Thus, the extrapolation to interior points of two numerically close parameterizations along the boundary provides similar results. In this way, the extrapolation based on GKPY equation is ‘‘stable’’ in the Hadamard sense, being a very suitable framework to perform the analytic continuation into the complex plane of the $\pi\pi$ scattering amplitude.

In Table IV, we collect the $f_0(500)$ pole parameters obtained from the extrapolation to the complex plane of the GKPY equations, using as input each of the different parameterizations described in Sec. II. The errors have been computed using a Monte Carlo Gaussian sampling of the corresponding parameterizations parameters with 7000 samples distributed within 3 standard deviations. As seen from Table IV, the differences between the pole values are smaller than 1%, proving the extremely small

		v_1	v_2	v_3	v_4	v_5
	$\pi^0\pi^0$	0.53	0.64	0.61	0.53	0.50
FDR	$\pi^+\pi^0$	0.43	0.43	0.43	0.43	0.43
	$I_{t=1}$	0.22	0.23	0.21	0.23	0.23
	S0	0.23	0.28	0.26	0.21	0.22
GKPY	S2	0.55	0.50	0.53	0.76	0.61
	P	0.11	0.08	0.10	0.22	0.13
Average		0.28	0.30	0.29	0.37	0.29

TABLE III: Average discrepancies \bar{d}_a^2 for each dispersion relation obtained with different versions of the CFD approach.

	$\sqrt{s_\sigma}$ (MeV)
v_1	$(457 \pm 14) - i(279 \pm 11)$
v_2	$(456 \pm 13) - i(278 \pm 12)$
v_3	$(457 \pm 13) - i(279 \pm 11)$
v_4	$(456 \pm 13) - i(280 \pm 11)$
v_5	$(456 \pm 14) - i(280 \pm 11)$

TABLE IV: $f_0(500)$ pole positions obtained from the analytic continuation to the complex plane of GKPY equations for each of the different parameterizations detailed in Sec. II.

dependence of the GKPY equations on the particular parameterization choice.

V. POLE DETERMINATION FROM PADÉ APPROXIMANTS

Padé Theory has been recently considered in Refs. [13, 14] as a tool for extracting resonance pole parameters through the analytic continuation of the elastic scattering amplitude². These works investigated the extraction of the mass, width and residue of the resonances using the well-known convergence properties of Padé approximants (PA) [26].

The approximant denoted as $P_M^N(s, s_0)$ is a rational function with a contact to the function to be approximated of order $N + M + 1$ at s_0 . It is given by the ratio of a polynomial of degree N over another of degree M . That means that the expansion of the PA around s_0 co-

incides with the expansion of the function up to the term of $\mathcal{O}((s - s_0)^{N+M})$.

Under quite general conditions [26], convergence is achieved when $N, M \rightarrow \infty$. In this regard, Padé Theory provides a toolkit [13, 14] that allows not only to propose a model-independent method for extracting resonance properties but also to provide a criterion for the evaluation of the theoretical error on the extraction of such resonance parameters. In particular, thanks to the Montessus de Ballore theorem [27] one is able to unfold the second Riemann sheet of a physical amplitude to search for the position of its resonance poles (if any) in the complex plane³.

To be more concrete, Montessus' theorem states that if a function $F(s)$ is analytic inside the disk $B_\delta(s_0) \equiv \{s | |s - s_0| < \delta\}$ except for a single pole at $s = s_p$, the sequence of one-pole Padé approximants $P_1^N(s, s_0)$ at s_0 ,

$$P_1^N(s, s_0) = \sum_{k=0}^{N-1} a_k (s - s_0)^k + \frac{a_N (s - s_0)^N}{1 - \frac{a_{N+1}}{a_N} (s - s_0)}, \quad (21)$$

converges to $F(s)$ in any compact subset of the disk excluding the pole s_p , i.e.,

$$\lim_{N \rightarrow \infty} P_1^N(s, s_0) = F(s). \quad (22)$$

As an extra consequence of this theorem, one finds that the PA pole $s_p^{PA} = s_0 + \frac{a_N}{a_{N+1}}$ converges to s_p for $N \rightarrow \infty$. The PA coefficients a_k are obtained by matching at a given s_0 the expansion of the PA to the expansion of the amplitude $F(s) = \sum_{k=0}^{N+1} a_k (s - s_0)^k + \mathcal{O}((s - s_0)^{N+2})$. If experimental data on the function to be approximated are available along a certain interval, the coefficients a_k can be obtained by a fit procedure. The use of the derivatives at a fixed point is, however, more robust if they are known with enough precision [14].

The Montessus' theorem can be generalized to a $P_M^N(s)$ sequence with $M \geq M^*$, where M^* is the number of poles of the original function $F(s)$. In this case, the rest of the poles inside the disk $B_\delta(s_0)$ are unphysical and may be viewed as artifacts that simulate other, more distant singularities, such as branch points produced by unitarity [28]. The next sequence following the Montessus' theorem would be the approximants with two poles, $P_2^N(s)$. In particular, each element of the $P_2^N(s, s_0)$ sequence around s_0 is given by (with the definition $a_k = 0$ for $k < 0$)

$$P_2^N(s, s_0) = \frac{\sum_{k=0}^N (a_k a_N^2 - a_k a_{N-1} a_{N+1} - a_{k-1} a_N a_{N+1} + a_{k-1} a_{N-1} a_{N+2} + a_{k-2} a_N^2 a_{N+1} - a_{k-2} a_N a_{N+2})(s - s_0)^k}{a_N^2 - a_{N-1} a_{N+1} + (a_{N-1} a_{N+2} - a_N a_{N+1})(s - s_0) - (a_N a_{N+2} - a_{N+1}^2)(s - s_0)^2}, \quad (23)$$

containing two poles located at

$$s_p^{PA} = s_0 + \frac{a_N a_{N+1} - a_{N-1} a_{N+2}}{2(a_{N+1}^2 - a_N a_{N+2})} \pm \frac{\sqrt{a_{N-1}^2 a_{N+2}^2 - 3a_N^2 a_{N+1}^2 + 4(a_{N-1} a_{N+1}^3 + a_N^3 a_{N+2}) - 6a_{N-1} a_N a_{N+1} a_{N+2}}}{2(a_{N+1}^2 - a_N a_{N+2})}. \quad (24)$$

One of the poles will converge to s_p for $N \rightarrow \infty$, while the other, together with the polynomial expansion, will simulate other structures.

From the above description, it follows that the precise extraction of the function and its higher derivatives at a given point s_0 is a necessary condition for the successful application of the method. In Ref [13], the amplitude $t_0^0(s)$ and its derivatives were obtained using the specific parameterization of the scalar isoscalar $\pi\pi$ phase shift $\delta_0^0(s)$ denoted as v_1 in Sec. II. In this section we extend the analysis to all the five parameterizations discussed in Sec. II. For each parameterization, we shall provide the central value of the resonance determination resulting from the central values of the input parameters, and the errors produced by the uncertainties from the input information and the truncation of the PA sequence. As in Eqs. (1) - (3), we will report the results for the pole position in terms of the mass and width of the resonance, defined by

$$\sqrt{s_p} = M - i\Gamma/2. \quad (25)$$

For the truncation error, denoted in [13] as “theoretical error”, we follow the criterium discussed in Refs. [13, 14] and adopt as estimator of the error the difference

$$\Delta\sqrt{s_p^N} = \left| \sqrt{s_p^N} - \sqrt{s_p^{N-1}} \right| \quad (26)$$

for both the mass M and the half-width $\Gamma/2$.

Using the central values and the higher derivatives for each parameterization given in Table II, we examined the convergence of the theoretical uncertainty (26) of the $P_1^N(s, s_0)$ for $N = 0, 1, 2, 3$ and of $P_2^N(s, s_0)$ with $N = 0, 1, 2$ for different PA centers s_0 in the adopted range of the elastic region (from $\pi\pi$ threshold to 0.85 GeV). The theoretical errors $\Delta\sqrt{s_p^3}$ and $\Delta\sqrt{s_p^2}$ for the $P_1^3(s, s_0)$ and $P_2^2(s, s_0)$, respectively, exhibit a minimum at a certain point s_0 , while the PA sequence is found to break down when s_0 approaches either the $\pi\pi$ threshold or the upper end of the considered range.

In order to incorporate the statistical uncertainties coming from the input error bands (Fig. 1), we use a

Monte Carlo simulation, where for a point s_0 we generate a set of phase shifts and derivatives $\{\delta^{(n)}(s_0)\}$, with a distribution according to their input errors (assumed to be uncorrelated). The Padé approximants $P_1^3(s, s_0)$ and $P_2^2(s, s_0)$ are then used to generate a distribution of pole positions.

The procedure is repeated for each s_0 and an optimal point, denoted as s_0^{opt} , is selected in such a way that the quadratic sum of the theoretical and statistical errors of M and $\Gamma/2$ is minimized. The obtained values of $\sqrt{s_0^{\text{opt}}}$ range from 470 MeV to 510 MeV for $P_1^3(s)$ and from 390 MeV to 510 MeV for $P_2^2(s)$. The theoretical error induced by the truncation of the PA sequence is of the same order as the uncertainties that stem from the statistical uncertainties of the phase shift.

After constructing the $P_1^3(s, s_0^{\text{opt}})$ and $P_2^2(s, s_0^{\text{opt}})$ for each parameterization, we extract their pole positions given by the central values of input parameters and collected them in the second column in Tables V and VI. The total error (fifth column) is given by the quadratic sum of the truncation theoretical error (third column) derived from (26) and the statistical error from the Monte Carlo simulation (fourth column), which are assumed Gaussian. We computed also the mean value of the statistical Monte Carlo distribution, which turned out to be comparable with the results in the second column (with deviations below 1 MeV), serving as a cross-check of the normality of the distribution.

Figs. 2 and 3 show the PA results in comparison with a reference value, taken as the prediction (2) of the GKPY equation. The last panels in Figs. 2 and 3 overlap the 68%CL predictions for the pole position from the different parameterizations. The spread of the results illustrate the instability of the analytic continuation: the different parameterizations are almost indiscernible in the physical region and satisfy to the same accuracy the dispersive constraints, but lead to rather different pole positions. This shows that choosing a particular parameterization leads to an underestimate of the theoretical uncertainty of the method.

The problem is to define a more realistic error estimate using these different determinations. The basic principle, considered also in previous works [15, 29], is to take into account the spread of the results obtained with indiscernible input in the physical region. But of course a unique prescription does not exist and some educated guess is necessary. The most conservative strategy would be to take into account the spread of the results seen in the 68%CL domains shown in the last panels of Figs. 2 and 3. Taking the extremes of the 1 standard deviation

² Analogous analyses have studied the extraction of the resonance poles through Laurent [24] and Laurent+Pietarinen expansions [25].

³ Further details such as the theorem proof and other extensions can be found in the book of Baker and Grave-Morris [26].

TABLE V: Mass and width (in MeV) for the $P_1^3(s)$ approximant.

	pole	theo. error	stat. error	combined error
v_1	$M = 452.8$	14.0	10.1	17.3
$(\sqrt{s_0} = 500)$	$\Gamma/2 = 296.8$	14.0	10.6	17.6
v_2	$M = 443.0$	12.3	7.2	14.3
$(\sqrt{s_0} = 510)$	$\Gamma/2 = 306.8$	12.3	7.2	14.2
v_3	$M = 456.6$	8.0	5.1	9.5
$(\sqrt{s_0} = 490)$	$\Gamma/2 = 303.2$	8.0	8.0	11.3
v_4	$M = 471.5$	12.9	5.7	14.1
$(\sqrt{s_0} = 470)$	$\Gamma/2 = 278.7$	12.9	9.4	16.0
v_5	$M = 463.8$	10.7	9.6	14.4
$(\sqrt{s_0} = 490)$	$\Gamma/2 = 291.7$	10.7	14.6	18.1

TABLE VI: Mass and width (in MeV) for the $P_2^2(s)$ approximant.

	pole	theo. error	stat. error	combined error
v_1	$M = 463.8$	8.8	13.5	16.1
$(\sqrt{s_0} = 390)$	$\Gamma/2 = 290.2$	8.8	8.4	12.1
v_2	$M = 455.6$	8.5	8.4	11.9
$(\sqrt{s_0} = 390)$	$\Gamma/2 = 291.5$	8.5	6.2	10.6
v_3	$M = 459.9$	7.2	6.6	9.8
$(\sqrt{s_0} = 470)$	$\Gamma/2 = 303.3$	7.2	4.9	8.8
v_4	$M = 477.0$	7.5	9.4	12.0
$(\sqrt{s_0} = 510)$	$\Gamma/2 = 288.2$	7.5	6.0	9.6
v_5	$M = 471.6$	10.5	11.4	15.6
$(\sqrt{s_0} = 390)$	$\Gamma/2 = 289.5$	10.5	7.7	13.1

ranges derived from Tables V and VI, we obtain for the P_1^3 and the P_2^2 sequences the error intervals:

$$M = (457 \pm 28) \text{ MeV}, \quad \Gamma/2 = (292 \pm 29) \text{ MeV}, \quad (27)$$

$$M = (466 \pm 23) \text{ MeV}, \quad \Gamma/2 = (294 \pm 18) \text{ MeV}. \quad (28)$$

Another possibility would be to include, besides the theoretical and statistical errors given in Tables V and VI, an additional uncertainty obtained from the spread of the central predictions of the various parameterizations. This prescription has the advantage of treating separately the various sources of error. The final central result will be then defined as the average of the individual central predictions and the error will be obtained as the quadratic sum of the three independent types of error. This procedure leads to slightly smaller errors than in (27,28), namely

$$\begin{aligned} M &= (457 \pm 14 \pm 14 \pm 10) \text{ MeV} = (457 \pm 22) \text{ MeV}, \\ \Gamma/2 &= (293 \pm 14 \pm 14 \pm 15) \text{ MeV} = (293 \pm 25) \text{ MeV}, \end{aligned} \quad (29)$$

for P_1^3 sequence and

$$\begin{aligned} M &= (466 \pm 11 \pm 11 \pm 14) \text{ MeV} = (466 \pm 21) \text{ MeV}, \\ \Gamma/2 &= (296 \pm 8 \pm 11 \pm 8) \text{ MeV} = (296 \pm 16) \text{ MeV}, \end{aligned} \quad (30)$$

for the P_2^2 determination. The three errors in the middle part of the identities are the parametrization, the truncation and the statistical uncertainties, respectively.

Both approximants give results for the mass and the width compatible with Eq. (2), with larger errors. The P_2^2 approximants lead to smaller parametrization, truncation and statistical errors. This may be due to the fact that the expression of the pole of the P_2^2 approximant in (24) uses all the input information (all the derivatives at s_0), while the pole of the P_1^3 approximant exclusively depends on the ratio of the last two derivatives, which in our case have the largest errors. Likewise, P_2^2 has an extra pole, having this PA sequence a larger flexibility and allowing a better approximate description of other singularities of the amplitude, like, e.g. the unitarity branch points.

VI. SUMMARY AND CONCLUSIONS

The problem investigated in this paper is the determination of resonances by using the method of Padé approximants to perform the analytic continuation of the scattering amplitude in the complex energy plane. We considered in particular the determination of the $f_0(500)$ resonance in $\pi\pi$ scattering, which is a notoriously difficult case since the associated pole is situated far from the real axis. Our analysis is a continuation of the work reported

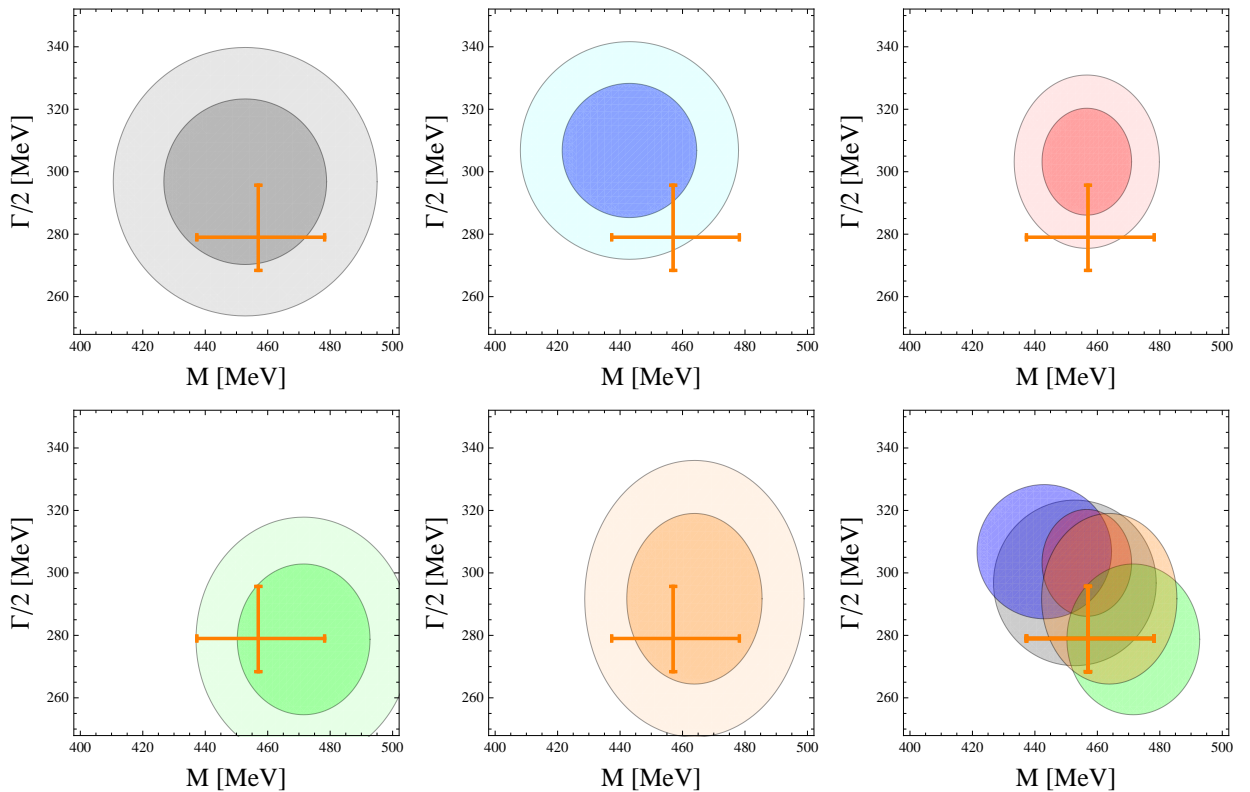


FIG. 2: Uncertainty regions for the $P_1^3(s, s_0)$ pole determination for each parameterization. Inner ellipses: 68%CL; outer ellipses: 95%CL. Orange cross: Eq. (2) shown to guide the eye. Last panel is the overlap of the 68%CL ellipses.

in [13], having as aim a more detailed investigation of the uncertainties of the pole determination.

The method of Padé approximants requires as input the value of the amplitude and its higher derivatives at a certain point s_0 [26]. In [13] these values were extracted from a specific parameterization of the S_0 wave, denoted in [10] as CFD, which describes with precision the experimental data and obeys a set of dispersive constraints. In order to assess more realistically the uncertainty of the method, we considered a set of admissible parameterizations which satisfy with accuracy the same constraints. The class described in Sec. II is quite general: all parameterizations are at least as good as CFD from the point of view of analyticity and unitarity. Just as CFD, they generalize the effective range approximation, extending its applicability to a larger domain of the complex energy plane. Moreover, all the parameterizations satisfy with very high precision the dispersive constraints on the cut, being equally good candidates as input for the determination of the lowest resonance. We used this class of functions both in the extrapolation by means of GKPY (Roy-type) equations and in the method of Padé approximants. From the spread of the pole predictions yielded by these parameterizations, we obtained a better estimate of the uncertainties of the mass and width of the resonance.

Actually, the errors derived by this approach are strictly speaking only lower bounds on the true uncertainty, since we restricted the admissible class to a limited set of specific parameterizations⁴. However, there are no many ways to impose unitarity in the elastic region, and the class of functions considered in the analysis is rather representative from the theoretical point of view. So, we assume that it allows a reasonable estimate of the uncertainty.

Our final predictions are given in Table IV for the extrapolation based on GKPY equations and in Eqs. (27,28) and (29,30) for the extrapolation based on Padé approximants. Our safest estimate, with largest errors, is given by the most conservative approach applied to the P_1^3 sequence in Eq. (27),

$$M = (457 \pm 28) \text{ MeV}, \quad \Gamma/2 = (292 \pm 29) \text{ MeV}. \quad (31)$$

The Roy-type integral representation leads to almost identical predictions for all parameterizations, therefore the error given in the original GKPY result (2) is not modified. On the other hand, the outcome of the direct

⁴ A parametrization-free approach (see Ref. [30] for an example) requires more complicated techniques of functional analysis.

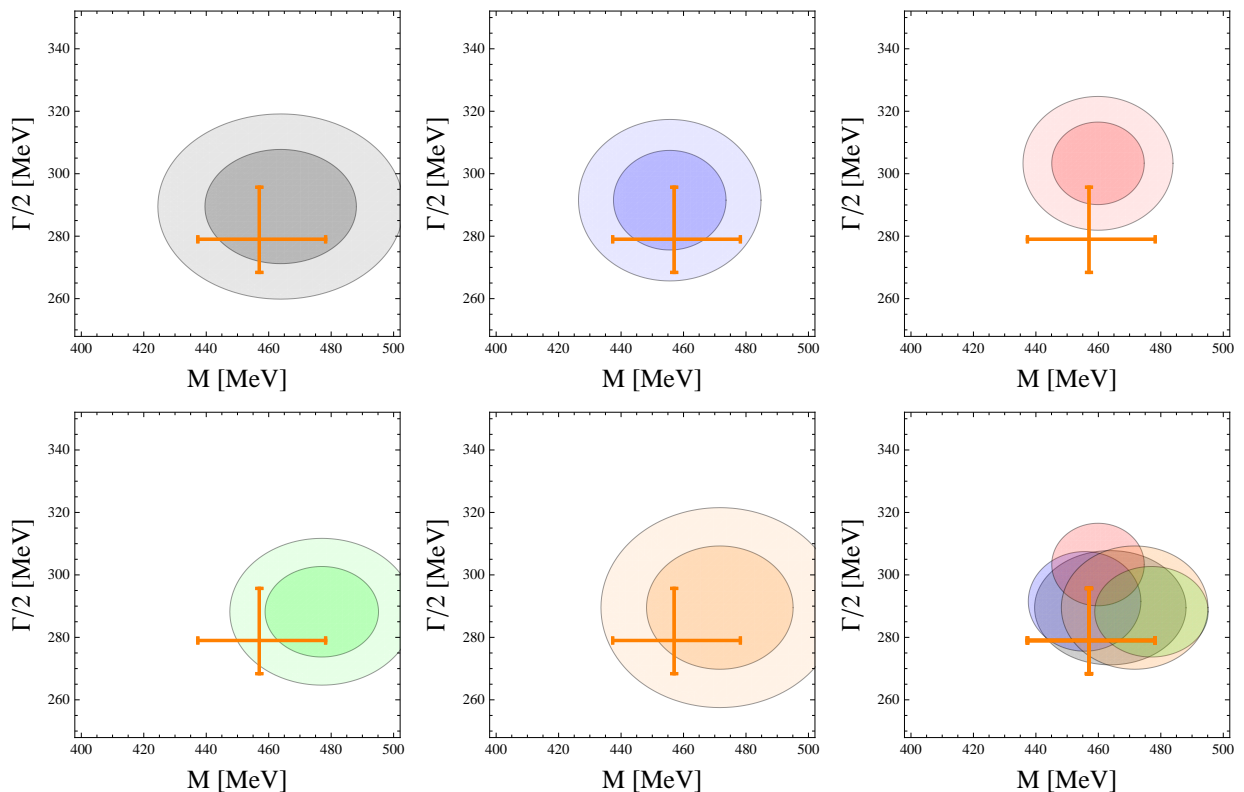


FIG. 3: Uncertainty regions for the $P_2^2(s, s_0)$ pole determination for each parameterization. Inner ellipses: 68%CL; outer ellipses: 95%CL. Orange cross: Eq. (2). Last panel is the overlap of the 68%CL ellipses.

analytic continuation through Padé approximants has a larger spread. This spread defines a new source of error, related to the instability of analytic continuation of functions almost indiscernible in the physical region. The origin of the larger errors lies in the higher derivatives of the function, used as input in the Padé approximants. The higher derivatives are not controlled by the constraints of unitarity and analyticity, and can be quite different for functions which satisfy with the same accuracy the dispersive constraints. These differences play a crucial role in the extrapolation to the pole in the complex plane.

Compared with the values given in Table IV, the most conservative result given in (31) has an error larger by a factor of about two. On the other hand, it is important to emphasize that the intervals provided by the Padé approximants in (27)-(30) are perfectly consistent within errors with the precise values obtained with the Roy-type integral representation. This gives confidence in the method.

In this work we have not further explored other possible approaches to reduce the Padé uncertainties. The aim of this work was to restudy the outcome of [13] which relied on the value of the phase-shift $\delta(s_0)$ and its first four derivatives $\delta^{(n)}(s_0)$. Considering additional derivatives would allow us to reach higher orders in the PA sequence and to decrease the truncation error. However, the sta-

tistical uncertainty is expected to increase. The study of the global error may tell if this can lead to a neat improvement. The incorporation of the precise knowledge on the scattering lengths [5, 10] can be also used to stabilize the Padé approximants and their pole prediction. Other approach that can be explored in future works consists on using directly the outcome $\text{Re } t_0^0(s)$ from the GKPY dispersion relation for the construction of the PA, which is expected to decrease the impact of the parametrization ambiguity. Our conclusions can be applied to the methods discussed in Refs. [24, 25] as well.

We recall finally that for constructing the Padé approximants we resorted as in [13] to the precise information on the S_0 partial wave provided by the dispersive constraints. Actually, in the case of $\pi\pi$ scattering the use of Padé approximants might seem unnecessary, since the straightforward analytic continuation of Roy or Roy-type equations offers the most precise way of finding the low-energy resonances [8–10]. However, by identifying the origin of the instability of the analytic continuation and by assessing in a more exhaustive way the uncertainties of Padé approximants, the investigation performed in this work provides a common methodology for the analysis of further reactions and observables, for which dispersive techniques cannot be applied but which can be addressed by means of the Padé approximant method.

Acknowledgments

The work of IC was supported by UEFISCDI under Contract Idei-PCE No 121/2011. The work of PM and JRE was supported by the Deutsche Forschungsgemeinschaft DFG through the Collaborative Research Center “The Low-Energy Frontier of the Standard Model” (SFB

1044) and “Subnuclear Structure of Matter” (SFB/TR 16) respectively. The work of JJSC was supported by the Spanish Ministry MINECO under grant FPA2013-44773-P, Consolider-Ingenio CPAN CSD2007-00042 and the Centro de Excelencia Severo Ochoa Programme under grant SEV-2012-0249.

-
- [1] K.A. Olive *et al.* (Particle Data Group), *Chin. Phys. C* **38**, 090001 (2014).
- [2] J.R. Pelaez, *From controversy to precision on the sigma meson: a review on the status of the non-ordinary $f_0(500)$ resonance*, arXiv:1510.00653.
- [3] J. Hadamard, *Lectures on Cauchy’s Problem in Linear Partial Differential Equations*, Dover, New York (1952).
- [4] S. Ciulli, C. Pomponiu and I. Sabba-Stefanescu, *Phys. Rep.* **17**, 133 (1975).
- [5] G. Colangelo, J. Gasser and H. Leutwyler, *Nucl. Phys.* **B603**, 125 (2001), hep-ph/0103088.
- [6] B. Ananthanarayan, G. Colangelo, J. Gasser, and H. Leutwyler, *Phys. Rept.* **353**, 207 (2001), hep-ph/0005297.
- [7] S.M. Roy, *Phys. Lett.* **B36**, 353 (1971).
- [8] I. Caprini, G. Colangelo and H. Leutwyler, *Phys. Rev. Lett.* **96**, 132001 (2006), hep-ph/0512364.
- [9] B. Moussallam, *Eur. Phys. J. C* **71**, 1814 (2011), arXiv:1110.6074 [hep-ph].
- [10] R. Garcia-Martin, R. Kaminski, J.R. Pelaez, J. Ruiz de Elvira, F.J. Yndurain, *Phys.Rev. D* **83**, 074004 (2011), arXiv:1102.2183 [hep-ph].
- [11] J. R. Batley *et al.*, (NA48/2 Collaboration), *Eur. Phys. J. C* **54**, 411 (2008).
- [12] R. Garcia-Martin, R. Kaminski, J. Pelaez and J. Ruiz de Elvira, *Phys. Rev. Lett.* **107**, 072001 (2011), arXiv:1107.1635 [hep-ph].
- [13] P. Masjuan, J. Ruiz de Elvira, J.J. Sanz-Cillero, *Phys. Rev. D* **90**, 097901 (2014), arXiv:1410.2397 [hep-ph].
- [14] P. Masjuan and J. J. Sanz-Cillero, *Eur. Phys. J. C* **73** (2013) 2594 arXiv:1306.6308 [hep-ph].
- [15] I. Caprini, *Phys. Rev. D* **77**, 114019 (2008), arXiv:0804.3504 [hep-ph].
- [16] A. Schenk, *Nucl. Phys.* **B363**, 97 (1991).
- [17] I. Caprini, G. Colangelo and H. Leutwyler, *Eur. Phys. J. C* **72**, 1860 (2012), arXiv:1111.7160 [hep-ph].
- [18] G.F. Chew and S. Mandelstam, *Phys. Rev.* **119**, 467 (1960).
- [19] P. Buettiker, S. Descotes-Genon and B. Moussallam, *Eur. Phys. J. C* **33**, 409 (2004) hep-ph/0310283.
- [20] M. Hoferichter, J. R. de Elvira, B. Kubis and U. G. Meißner, arXiv:1510.06039 [hep-ph].
- [21] Hyams, B., *et al.*, *Nucl. Phys.* **B64**, 134, (1973); Estabrooks, P., and Martin, A. D., *Nucl. Physics*, **B79**, 301, (1974); Protopopescu, S. D., *et al.*, *Phys Rev.* **D7**, 1279, (1973); Kamiński, R., Lesniak, L, and Rybicki, K., *Z. Phys.* **C74**, 79 (1997) and *Eur. Phys. J. direct* **C4**, 1 (2002); Hyams, B., *et al.*, *Nucl. Phys.* **B100**, 205, (1975); Losty, M. J., *et al.* *Nucl. Phys.*, **B69**, 185 (1974); Hoogland, W., *et al.* *Nucl. Phys.*, **B126**, 109 (1977); Durusoy, N. B., *et al.*, *Phys. Lett.* **B45**, 517 (1973).
- [22] Grayer, G., *et al.*, *Nucl. Phys.* **B75**, 189, (1974).
- [23] R. Navarro Pérez, E. Ruiz Arriola and J. Ruiz de Elvira, *Phys. Rev. D* **91**, 074014 (2015) arXiv:1502.03361 [hep-ph].
- [24] Z. H. Guo and J. A. Oller, arXiv:1508.06400 [hep-ph].
- [25] A. Svarc, M. Hadzimehmedovic, H. Osmanovic, J. Stahov, L. Tiator and R.L. Workman, *Phys. Rev. C* **88**, no. 3, 035206 (2013) arXiv:1307.4613 [hep-ph].
- [26] G.A.Baker and P. Graves-Morris, *Padé Approximants*, edited by C. U. Press (Encyclopedia of Mathematics and its Applications, 1996).
- [27] R. de Montessus de Ballore, *Bull. Soc. Math. France* **30**, 28 (1902).
- [28] P. Masjuan, J. J. Sanz-Cillero and J. Virto, *Phys. Lett. B* **668** (2008) 14 arXiv:0805.3291 [hep-ph].
- [29] R. Garcia-Martin, J.R. Pelaez and F.J. Yndurain, *Phys. Rev. D* **76**, 074034 (2007).
- [30] I. Caprini, S. Ciulli, A. Pomponiu, I. Sabba-Stefanescu, *Phys. Rev. D* **5**, 1658 (1972).